Impact of Random Telegraph Noise with Various Time Constants and Number of States in CMOS Image Sensors

Rihito Kuroda [a], Akinobu Teramoto [b] and Shigetoshi Sugawa [a,b]
[a] Graduate School of Engineering, Tohoku University,
[b] New Industry Creation Hatchery Center, Tohoku University
6-6-11-811, Aza-Aoba, Aramaki, Aoba-ku, Sendai, Miyagi, Japan 980-8579
TEL: +81-22-795-4833, FAX: +81-22-795-4834, Email address: rihito.kuroda.e3@tohoku.ac.jp

ABSTRACT

In this work, the impact of random telegraph noise (RTN) with various time constants and number of states to noise characteristics of CMOS image sensors are summarized based on a statistical measurement and analysis of a large number of MOSFETs. The obtained results suggest that from a trap located relatively away from the gate insulator/Si interface, the trapped carrier is emitted to the floating diffusion (FD) node. Also, an evaluation of RTN using root mean square values tends to underestimate the effect of RTN with large amplitude and relatively long time constants or multiple states. It is proposed that the amplitude of noise should be incorporated during the evaluation.

INTRODUCTION

Detection, characterization and reduction of random telegraph noise (RTN) are critically important in CMOS image sensors (CIS)[1]. A transition of the trap state (filled or empty) of in-pixel source follower (SF) during correlated double (CDS) sampling generates RTN in CIS. RTN induces relatively large noise amplitude at fixed pixels, and the visibility of RTN in captured images is quite significant. Especially for CIS with sub-electron readout noise, RTN becomes a stumbling block to achieve photon-countable sensitivity with all the pixels[2]. By using the array test circuit, we have previously reported statistical analysis of RTN regarding the effects of device structures, process conditions, detailed analysis of time constants and so on[3-8]. The parameters of RTN include amplitude, time constants (time to capture, τ_c and time to emission, τ_e,) and number of states, and these parameters vary significantly among transistors. For example, measurement results of RTN with sampling period of 1μs and sampling time of 600s revealed that the time constants ratio ($<\tau_c>/<\tau_e>$) in two-state RTN is distributed for at least nine order of magnitude[6]. Also, various types of multi-state RTN incorporated with multiple number of traps in a transistor have been reported to appear[7]. The effect of RTN during CIS operation may also vary due to the different sets of RTN parameters. For CIS in general, the effect of RTN is evaluated by the measured values of root mean square of pixel output signal after CDS. The effect of RTN with various parameters to the readout noise of CIS has not been fully studied. Recently, an extraction method of characteristic time constants of RTN (τ_s) based on double sampling has been reported to be useful[9]. In this work, we describe the impact of RTN with various time constants and number of states in CIS operation using CDS in order to clarify the effects of RTN with various parameters and propose an evaluation method thereof. Distribution of time constants and their behavior to gate overdrive voltage are summarized first. Then, using the waveforms obtained by fast and long sampling (1μs period for 600s) of MOSFETs with RTN, noise characteristics in CDS operation with various sampling intervals and sampling numbers were analyzed and important findings are summarized.

EXPERIMENTAL SETUP

Fig.1 shows the test circuit used in this work to statistically analyze the RTN characteristics[3-8]. Fig.2 shows the block diagram of measurement system. Fig.3 summarizes the experimental procedure in this work. The array test circuit was fabricated by a 0.22μm technology node CMOS technology. The gate oxide thickness and gate size (width/length) of measured MOSFETs are 5.6nm and 0.28μm/0.22μm, respectively. At first, output signal of 131K MOSFETs were measured by non-CDS frame sampling to extract MOSFETs with RTN waveforms. Then, for randomly selected 721 MOSFETs with RTN, non-CDS continuous sampling was carried

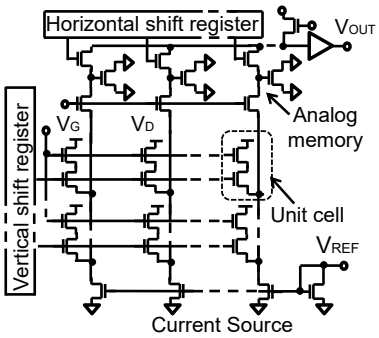

Fig.1 Test circuit to statistically characterize RTN of in-pixel SF.

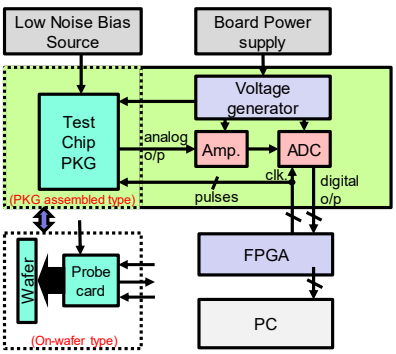

Fig.2 Block diagram of measurement system.

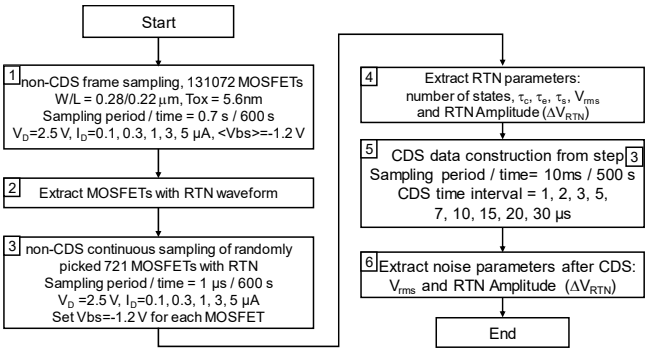

Fig.3 Experimental procedure in this work. CDS waveform was constructed by measured continuous sampling data.

out for each MOSFET with 1μs sampling period for 600s and the parameters of RTN were extracted. After that, the CDS waveforms with various time intervals and sampling numbers were constructed from the obtained non-CDS raw data, and the noise parameters such as root mean square of pixel output voltage (V_{rms}) and maximum RTN amplitude (ΔV_{RTN}) were extracted to be analyzed.

RESULTS AND DISCUSSIONS

Fig.4 shows the cumulative probability distribution of V_{rms} of 131K MOSFETs with five drain current (I_D) conditions measured at the step 1 in Fig.3. RTN waveforms appeared in about 10% of measured MOSFETs. As previously reported, appearance probability of high V_{rms} due to RTN is reduced by increasing the drain current. It is because the effect of a trap becomes smaller when the number of carriers in channel is larger. Fig.5 shows the ratio of number of RTN states for the measured MOSFETs under non-CDS continuous sampling extracted at the step 4 in Fig.3. About 40% of the measured MOSFETs with RTN in this work exhibited more than two states under the measurement condition. This suggests the impact of multi-state RTN toward CIS noise characteristics should be paid attention. Fig.6 shows the extracted mean time to capture $<\tau_c>$ as a function of mean time to emission $<\tau_e>$. They are distributed broadly for at least six orders of magnitude from several micro seconds to several seconds[6]. Fig.7 shows the dependencies of $<\tau_c>$ and $<\tau_e>$ on the V_{GS} for extracted 35 MOSFETs[5], and Fig.8 shows the energy band diagrams with capture and emission processes to explain the results in Fig.7. In Fig.7(a), $<\tau_c>$ decreases exponentially as V_{GS} increases for all of the extracted MOSFETs. When V_{GS} increases, the channel electron density increases exponentially within the measured conditions. Then the capture probability, which is inversely proportional to $<\tau_c>$, increases exponentially[5]. The dependency of $<\tau_e>$ on V_{GS} is categorized into three types as shown in Fig.7(b-d). Here, $<\tau_e>$ depends on the distance and difference of energy levels between the trap and conduction band of substrate to which the carrier is emitted[4-5]. In Fig.7(b), $<\tau_e>$ increases as V_{GS} increases, it is because the potential barrier toward Si increases. In Fig.7(c), $<\tau_e>$ does not change, indicating the trap position is near the interface. The results in Fig.7(d), where $<\tau_e>$ decreases as V_{GS} increases, indicate that for a part of MOSFETs with relatively long $<\tau_e>$, i.e., located relatively away from the interface, trapped electrons are emitted to the poly-Si gate electrode side instead of Si channel side. This is especially problematic to CIS aiming for photon-countable sensitivity because the emitted electrons are mixed with signal electrons at the FD node. This may limit the thinning of the gate oxide of SF, which is effective to reduce RTN amplitude due to the gate capacitance increase.

Figs.9-10 show the relationship of V_{rms} and ΔV_{RTN} between continuous sampling and CDS modes for various numbers of CDS sampling. V_{rms} has long been employed as index of noise, however RTN with a large ΔV_{RTN} and a long time constant is underestimated for some applications like movie video capturing in low light level or it may be even undetected because of small V_{rms}. The ΔV_{RTN} is not suppressed by the CDS operation as indicated in Fig.10 if a capture or an emission occurs during the CDS interval. Fig.11 shows the waveforms, histograms and V_{rms} as a function of CDS interval for specific four samples A~D shown in Figs.9-10.

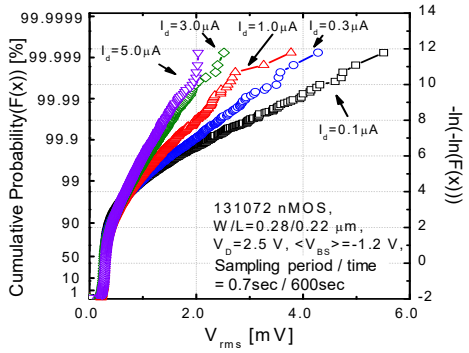

Fig.4 Cumulative probability of V_{rms} for five I_D conditions measured at the step 1 in Fig.3.

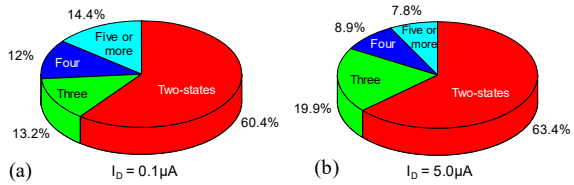

Fig.5 Pie chart of the number of RTN states for (a) I_D=0.1μA and (b) I_D=5.0μA, respectively.

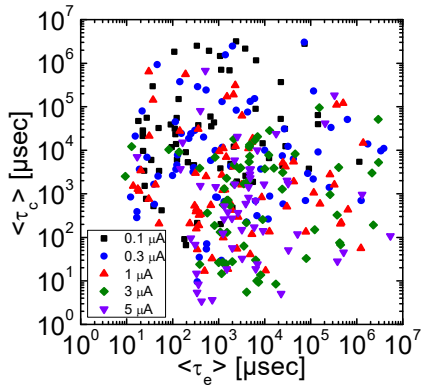

Fig.6 Distribution of measured $<\tau_e>$ and $<\tau_c>$. $<\tau_e>$ and $<\tau_c>$ are broadly distributed for at least six orders of magnitude.

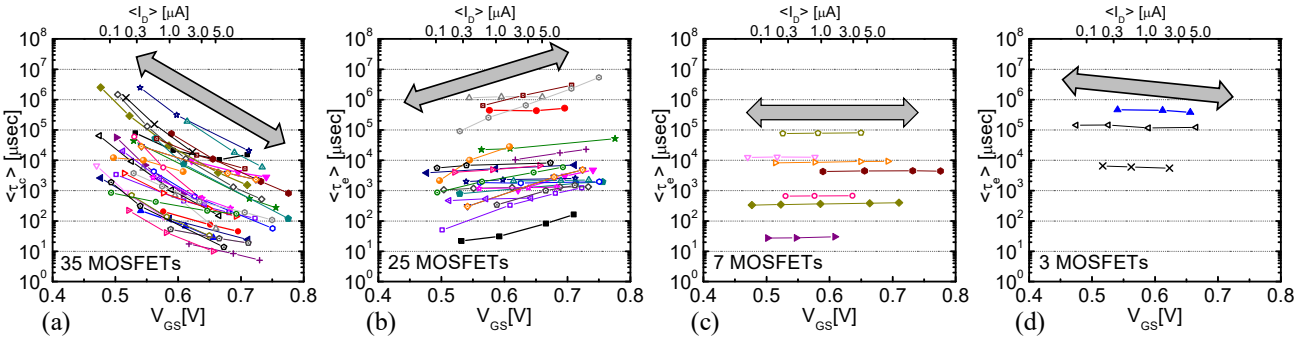

Fig. 7 (a) $<\tau_c>$ and (b-c) $<\tau_e>$ as functions of V_{GS}. $<\tau_c>$ for all the extracted MOSFETs follow the same dependency on V_{GS}, i.e., $<\tau_c>$ decreases exponentially as V_{GS} increases. For $<\tau_c>$, three dependencies were observed; in (b) $<\tau_c>$ increases, in (c) $<\tau_c>$ does not change and in (d) $<\tau_c>$ decreases as V_{GS} increases, respectively.

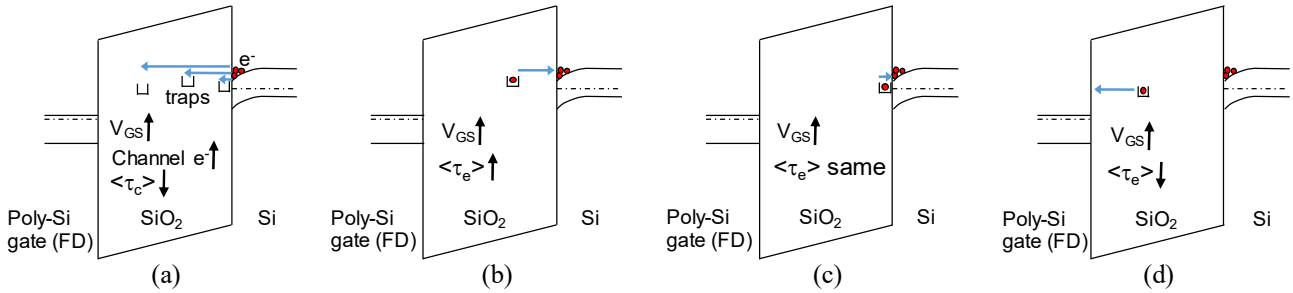

Fig. 8. Energy band diagrams with (a) capture and (b-c) emission processes of electrons due to traps to explain the results shown in Fig.7(a) though (b), respectively.

The characteristics of V_{rms} as a function of CDS interval are well fitted for two-state RTN cases by the following equation 1[9], which is a function of the time constants and ΔV_{RTN}.

$$V_{rms} = \frac{\sqrt{2\tau_e\tau_c}}{\tau_e+\tau_c}\cdot\Delta V_{RTN}\cdot\sqrt{1-\exp(-t/\tau_s)} \quad (1)$$

$$\tau_s = \frac{\tau_e\tau_c}{\tau_e+\tau_c} \quad (2)$$

For the sample D which shows multi-state RTN, its ΔV_{RTN} in CDS operation is determined by the direct transition between the most distant states. This cannot be characterized by taking into account the V_{rms} only. Consequently, for RTN with relatively long time constant as well as with multiple states, the ΔV_{RTN} should be taken into account together with the V_{rms} for characterization.

CONCLUSIONS

The impact of RTN with various time constants and number of states to noise characteristics of CIS were demonstrated in this work. It is suggested that from a trap located relatively away from the gate insulator/Si interface, the carrier is emitted to the FD node, which is to be mixed with signal photoelectrons. An evaluation of RTN using V_{rms} values tends to underestimate the effect of RTN with large amplitude and relatively long time constants or multiple states. It is proposed that the amplitude of noise should be incorporated for the evaluation of RTN. These findings are important for characterization and reduction of RTN. The effect of RTN in correlated multiple sampling will be studied based on the framework developed in this work.

REFERENCES

[1] X. Wang, M F. Snoeji, P. R. Rao, A. Mierop, A. J.P Theuwissen, "Random telegraph signal in CMOS image sensor pixels," IEDM, Tech. Dig., pp.115-118, 2006.

[2] M-W. Seo, S. Kawahito, K. Kagawa, K. Yasutomi, "A 0.27e⁻rms Read Noise 220-μV/e⁻ Conversion Gain Reset-Gate-Less CMOS Image Sensor With 0.11-μm CIS Process," IEEE EDL, Vol.36, No.12, pp.1344-1347, 2015.

[3] K. Abe, S. Sugawa, R. Kuroda, S. Watabe, N. Miyamoto, A. Teramoto, T. Ohmi, Y. Kamata, and K. Shibusawa, "Analysis of source follower random telegraph signal using nMOS and pMOS array TEG," Proc. IISW, pp. 62-65, 2007.

[4] A. Teramoto, F. Fujisawa, K. Abe, S. Sugawa and T. Ohmi, "Statistical Evaluation for Trap Energy Level of RTS Characteristics," Symp. VLSI Technology, Dig. Tech. Papers, pp.99-100, 2010.

[5] Y. Yonezawa, A. Teramoto, T. Obara, R. Kuroda, S. Sugawa, T. Ohmi, "The Study of Time Constant Analysis in Random Telegraph Noise at the Subthreshold Voltage Region," Proc. Intl. Reliability Phys. Symp., XT.11.1-6, 2013.

[6] T. Obara, A. Yonezawa, A. Teramoto, R. Kuroda, S. Sugawa, T. Ohmi, "Extraction of time constants ratio over nine orders of magnitude for understanding random telegraph noise in metal-oxide-semiconductor field-effect transistors," Jpn. J. Appl. Physics, Vol.53, pp.04EC19-1-7, 2014.

[7] T. Obara, A. Teramoto, A. Yonezawa, R. Kuroda, S. Sugawa and T. Ohmi, "Analyzing Correlation between Multiple Traps in RTN Characteristics," Proc. Intl. Reliability Phys. Symp., 4A.6.1-4A.6.7, 2014.

[8] R. Kuroda, A. Teramoto and S. Sugawa, "Rondom Telegraph Noise Measurement and Analysis based on Arrayed Test Circuit toward High S/N CMOS Image Sensors," Proc. Intl. Conf. Microelectronic Test Structures, pp.46-51, 2016.

[9] C. Y-P. Chao, H. TU, T. Wu, K-Y. Chou, S-F. Yeh, F-L. Hsueh, "CMOS Image Sensor Random Telegraph Noise Time Constant Extraction From Correlated To Uncorrelated Double Sampling," J. Electron Device Society, Vol.5, No.1 pp.79-89, 2017.

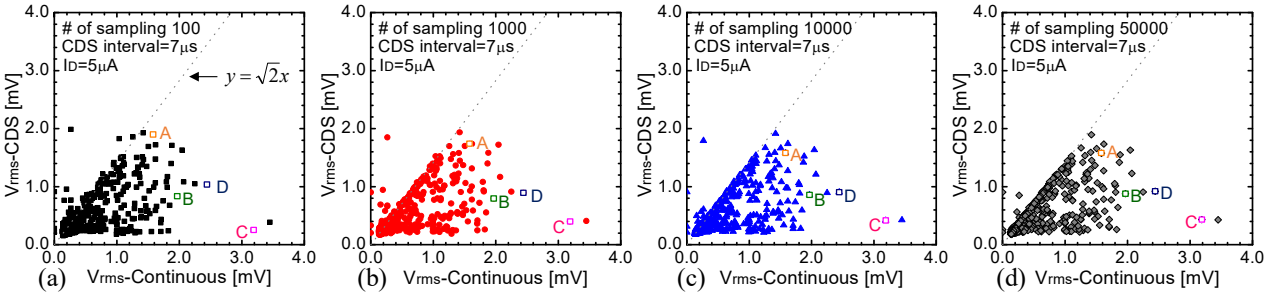

Fig.9 V_{rms} extracted in CDS with 7μsec interval and 10ms period as a function of V_{rms} extracted in continuous sampling for different CDS sampling numbers; (a) 100, (b) 1000, (c) 10000 and (d) 50000. Markers A~D indicate specific four MOSFETs.

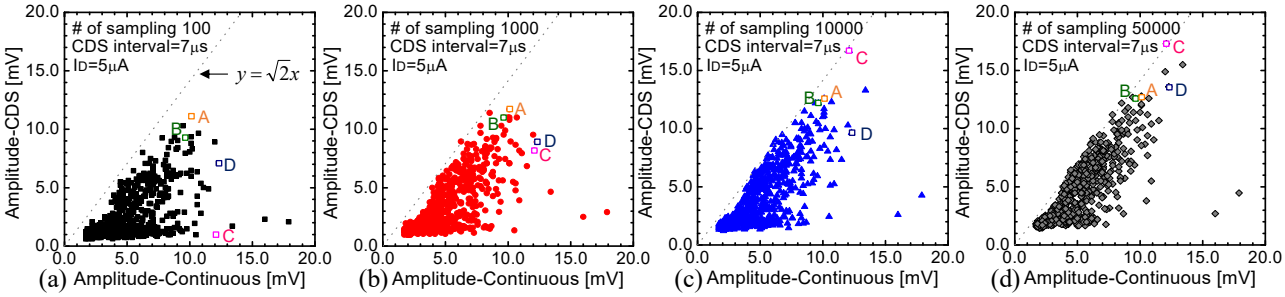

Fig.10 ΔV_{RTN} extracted in CDS with 7μsec interval and 10ms period as a function of ΔV_{RTN} extracted in continuous sampling for different CDS sampling numbers, (a) 100, (b) 1000, (c) 10000 and (d) 50000. Markers A~D indicates specific four MOSFETs. The ΔV_{RTN} in CDS increases as the sampling number increases and tends to reach the ΔV_{RTN} in continuous samping mode multiplied by squre root of two.

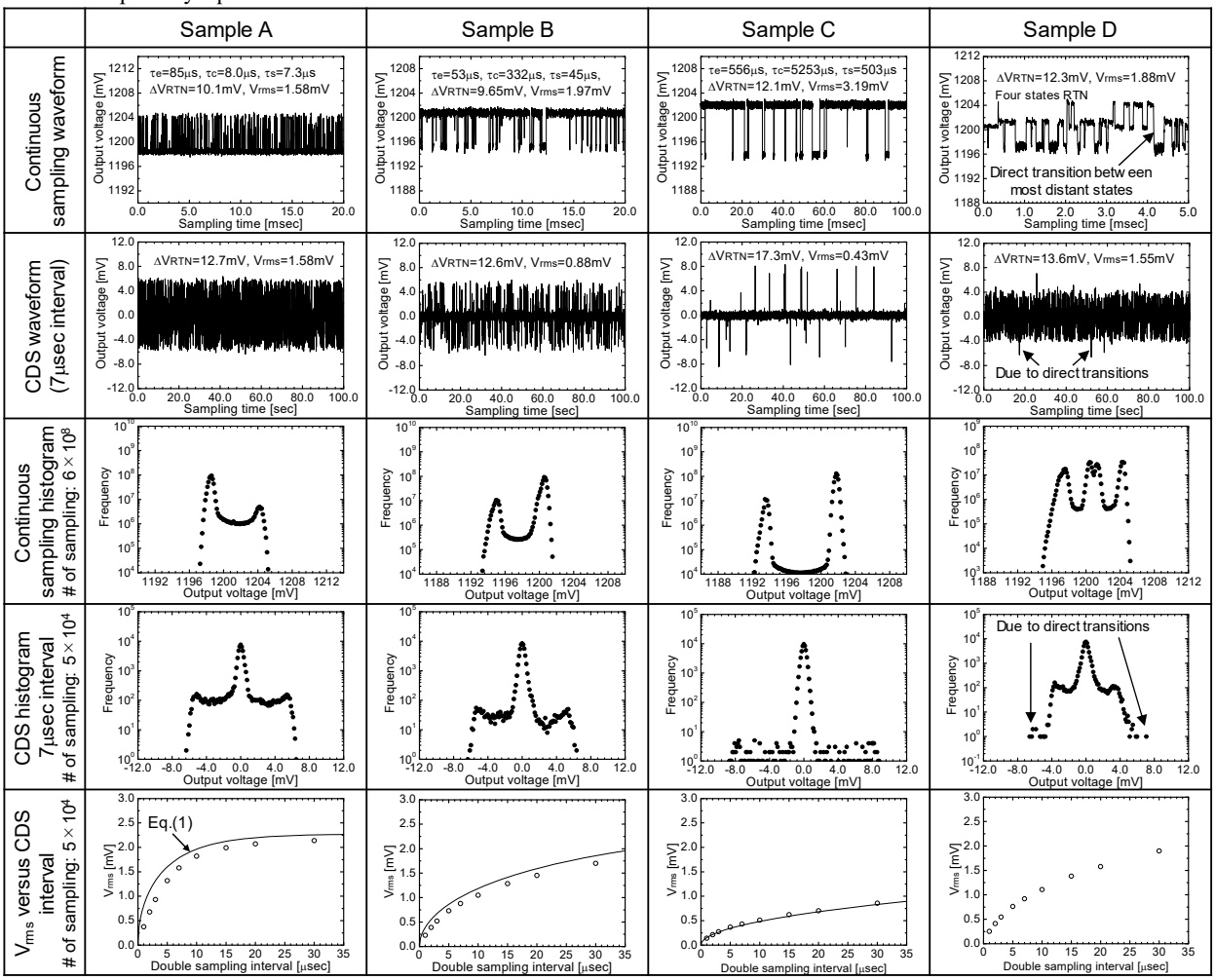

Fig.11 Waveforms and histogram in continuous sampling and CDS, and V_{rms} as functions of double sampling interval for samples A~D. Sample C exhibits a relatively long τ_s, thus V_{rms} in CDS becomes relatively small. However, the ΔV_{RTN} is as large as that of continuous sampling mode times square root of two when signal transition occur during the CDS interval.